BY LEE-LUENG FU, DUDLEY B. CHELTON, PIERRE-YVES LE TRAON, AND ROSEMARY MORROW

EDDY DYNAMICS FROM SATELLITE ALTIMETRY

ABSTRACT. Most of the kinetic energy of ocean circulation is contained in ubiquitous mesoscale eddies. Their prominent signatures in sea surface height have rendered satellite altimetry highly effective in observing global ocean eddies. Our knowledge of ocean eddy dynamics has grown by leaps and bounds since the advent of satellite altimetry in the early 1980s. A satellite's fast sampling allows a broad view of the global distribution of eddy variability and its spatial structures. Since the early 1990s, the combination of data available from two simultaneous flying altimeters has resulted in a time-series record of global maps of ocean eddies. Despite the moderate resolution, these maps provide an opportunity to study the temporal and spatial variability of the surface signatures of eddies at a level of detail previously unavailable. A global census of eddies has been constructed to assess their population, polarity, intensity, and nonlinearity. The velocity and pattern of eddy propagation, as well as eddy transports of heat and salt, have been mapped globally. For the first time, the cascade of eddy energy through various scales has been computed from observations, providing evidence for the theory of ocean turbulence. Notwithstanding the tremendous progress made using existing observations, their limited resolution has prevented study of variability at wavelengths shorter than 100 km, where important eddy processes take place, ranging from energy dissipation to mixing and transport of water properties that are critical to understanding the ocean's roles in Earth's climate. The technology of radar interferometry promises to allow wide-swath measurement of sea surface height at a resolution that will resolve eddy structures down to 10 km. This approach holds the potential to meet the challenge of extending the observations to submesoscales and to set a standard for future altimetric measurement of the ocean.

INTRODUCTION

In the early 1960s, swirls of ocean currents with spatial scales from tens to hundreds of kilometers and time scales from days to months were found to be the oceanic analog of storms in the atmosphere. The deployment of moored instruments and drifting floats in the open seas during the ensuing decade documented the ubiquity of such motions in the world's ocean. The term "mesoscale eddies" was established for these motions and associated variability of ocean properties (e.g., Robinson, 1983). The kinetic energy of ocean circulation is dominated by mesoscale eddies, which play a significant role in transporting water mass, heat, and nutrients in the ocean. Studying the dynamics governing mesoscale eddies has been a central theme of physical oceanography for decades.

Sparse distribution of in situ measurements limited detailed knowledge of the global pattern of mesoscale eddies. The launch of Earth-observing satellites in the late 1970s opened a new window for studying the surface characteristics of these energetic motions from a global perspective (see Le Traon and Morrow, 2001, for a review). Owing to their strong effects on sea surface properties, mesoscale eddies are easily seen on images of sea surface temperature and ocean color. However, water-surface-property signatures do not convey much information on the dynamic processes of eddies. Through geostrophic balance, water motions associated with eddies, as well as mean flows, are related to the departure of sea surface height (SSH) from the geoid, the surface on which Earth's gravity is constant. This height departure from the geoid is called ocean surface topography, which is related to the geostrophic velocity of ocean surface currents. To the extent that surface geostrophic velocity reflects an integral dynamic effect of the upper-ocean density field, SSH observations from a satellite radar altimeter are very effective for studying eddy dynamics on a global scale. SSH variability associated with mesoscale eddies creates the strongest signals from satellite radar altimeters. Although the performance of the first-generation altimeter of the GEOS-3 mission was quite poor, with orbit uncertainty larger than 1 m and instrument noise higher than 10 cm, the SSH variability associated with mesoscale eddies was clearly discernible in the noisy data (Huang et al., 1978).

The much improved Seasat altimeter provided the first map of global ocean mesoscale variability (Cheney et al., 1983; Fu, 1983), albeit the energy level was underestimated due to the short three-month duration of the mission. Based on Seasat technology, Geosat was developed and launched into an orbit that was selected to map ocean mesoscale eddies. Although Geosat did not carry instruments to correct for the delay of radar signal propagation caused by the effects of ionospheric free electrons and tropospheric water vapor, it provided the first opportunity to study the dynamic properties of mesoscale eddies on a global basis (Zlotnicki et al., 1989), especially in energetic regions where measurement errors did not overwhelm the signal.

The launch of European Remote Sensing Satellite-1 (ERS-1) and TOPEX/ Poseidon (T/P) initiated a new era for studying oceanic mesoscale eddies. T/P was designed specifically for observing SSH with sufficient accuracy and sampling to study large-scale changes in ocean circulation and sea level. Although the 2.8° spacing between its ground tracks (e.g., 315 km at the equator; 200 km at 50° latitude) is too large to resolve the two-dimensional structure of mesoscale eddies, the orbit of ERS-1 is a good complement to that of T/P. Its higher inclination allows coverage of the polar oceans up to 82° latitude, beyond the 66° limit of T/P. Its 35-day repeat period, as opposed to 10 days for T/P, corresponds to a much smaller ground track spacing of ~ 0.7°, which is about 80 km at the equator.

A data set has been created by merging the two altimeter data streams from T/P and ERS-1 with the use of objective analysis technique (Ducet et al., 2000). This data set, produced by and available from the French Archiving, Validation and Interpretation of Satellite Oceanographic (AVISO) data center, now covers 17 years, extending from the beginning of the T/P mission to the present by using data from each of the follow-on missions to T/P (Jason-1 and Ocean Surface Topography Mission/ Jason-2) and ERS-1 (ERS-2 and Envisat). The AVISO data set has provided a fertile ground for numerous studies of ocean circulation at spatial and temporal scales never observed before.

In this paper, we first review the progress made using satellite altimetry to advance knowledge of ocean mesoscale eddies, from early efforts to detect eddies to recent results of tracking the movement of eddies around the world's ocean. We also discuss the roles of eddies in energy, mass, and ocean property flux. We then discuss the limitations of the existing data in resolving the scales of

eddy motion and highlight the importance of the unresolved submesoscales. Finally, we address the challenges for developing the next-generation altimetry missions to observe ocean eddies.

STUDIES FROM ALONG-TRACK DATA

A major finding from the in situ observations made in the 1970s was the ubiquitous dominance of eddies in ocean variability. It was not surprising that the first ocean signals detected from satellite altimetry were from eddies. At the speed of 7 km s^{-1}, a satellite radar altimeter provides a snapshot of an SSH profile along its ground tracks, revealing the spatial structure of ocean variability that is not available from in situ observations. The SSH wavenumber spectrum, which conveys the distribution of SSH variance on spatial scales, has been a topic of investigation since the early days of satellite altimetry (Fu, 1983). Despite eddies' varying energy levels at different locations, their spectra at the high-wavenumber end exhibits a power law like k^{-p}, where k denotes wavenumber. The exponent p is interpreted as an indicator of the dynamic process governing eddy energy transfer in spectral space. Although eddy motions are in geostrophic balance, the governing dynamics are increasingly nonlinear at high wavenumbers, where the theory of geostrophic turbulence

(Charney, 1971) is expected to apply and dictates a k^{-3} spectrum for kinetic energy, or k^{-5} for SSH.

Based on three years' worth of T/P data, Stammer (1997) advocated for the existence of a normalized universal SSH wavenumber spectrum following the k^{-5} power law, consistent with the geostrophic turbulence theory. More recent studies have disputed this conclusion. Using multiple altimeter data sets, Le Traon et al. (2008) suggest that the SSH spectrum in high-eddy-energy regions is closer to $k^{-11/3}$ than to k^{-5} and is consistent with the theory of surface quasi-geostrophic turbulence that takes the effects of the surface boundary into consideration (a point further discussed in a later section on Flux of Oceanic Energy and Properties). Using data from the Jason-1 altimeter, Fu and Ferrari (2008) show that the spectrum in low-eddy-energy areas clearly follows k^{-2}. Therefore, as previously argued by Le Traon (1993), there does not seem to be a strong case for the existence of a universal wavenumber spectrum. Understanding the differences in spectral shape between low- and high-eddy-energy regions remains an open issue.

The tradeoff between spatial and temporal sampling of a single satellite altimeter makes it difficult to track the two-dimensional movement of ocean eddies. However, two-dimensional

information on eddy current velocity can be obtained at the crossover points of altimeter observations by combining the two cross-track components of eddy geostrophic velocity to estimate the velocity vector of eddy motions. Applying this approach to Geosat data, Morrow et al. (1994) constructed time series of eddy current velocity in the Southern Ocean where the density of crossover points is relatively high. They mapped the distribution of eddy velocity variance and correlation in terms of current ellipse as well as Reynolds stress. They also computed eddy momentum fluxes from these quantities and found that the forcing of eddies on mean flows is comparable to the magnitude of wind forcing.

After the launch of Jason-1, T/P was moved into a new orbit for a tandem mission with Jason-1. The new ground tracks of T/P were interleaved with those of Jason-1, which flew over the original T/P tracks (with 2.8° separation in longitude). The overflight times of the two satellites crossing a given latitude were nearly simultaneous (only seven minutes apart), allowing the along-track geostrophic velocity to be estimated directly from the SSH difference between the two measurements separated by 1.4° in longitude. This provided direct estimates of the large-scale geostrophic velocity vector along satellite tracks. Scharffenberg and Stammer (2010) compute the eddy kinetic energy from the tandem mission data and illustrate its dominance over the kinetic energy of the mean flow. Although the 1.4° cross-track separation leads to underestimation of the geostrophic velocity (Schlax and Chelton, 2003), the eddy kinetic energy is larger than the mean kinetic energy by

Lee-Lueng Fu *(lee-lueng.fu@jpl.nasa.gov) is Senior Research Scientist, Jet Propulsion Laboratory, California Institute of Technology, Pasadena, CA, USA.* **Dudley B. Chelton** *is Distinguished Professor of Oceanic and Atmospheric Sciences, College of Oceanic and Atmospheric Sciences, Oregon State University, Corvallis, OR, USA.* **Pierre-Yves Le Traon** *is Program Director, Operational Oceanography, Institut français de recherche pour l'exploitation de la mer, Centre de Brest, Plouzané, France.* **Rosemary Morrow** *is Assistant Physicist, Laboratoire d'Études en Géophysique et Océanographie Spatiales, Centre National d'Études Spatiales, Toulouse, France.*

more than an order of magnitude over most of the global ocean, confirming a well-known observation established by sparse in situ data decades ago.

MAPPING THE EDDY FIELD
Merged Observations From Multiple Altimeters

Launching multiple satellite altimeters to increase the spatial and temporal resolution was only an idea until the launch of T/P and ERS-1 provided the first opportunity to merge observations from two altimeters. Most mesoscale studies are now taking advantage of the improved resolution derived from the SSALTO/DUACS[1] merged, gridded data sets distributed by AVISO (Le Traon et al., 1998). Ducet et al. (2000) presented the first global high-resolution maps of mesoscale variability. Comparing the SSH wavenumber spectrum from the merged data to that from the along-track data, which was considered to represent the intrinsic resolution of the altimeter data, they estimated the resolution of the merged data to be about 150 km in wavelength. A similar resolution of about 2° in longitude by 2° in latitude has recently been inferred from wavenumber spectral analysis of the gridded SSH fields (Chelton et al., in press). For Gaussian-shaped eddies, this wavelength resolution corresponds to being able to detect mesoscale features with e-folding scales of about 0.4°. Displayed in Figure 1 is a snapshot of the SSH anomalies over the Pacific Ocean, illustrating the ubiquitous presence of eddies to the extent resolved by the combined observations from the two altimeters.
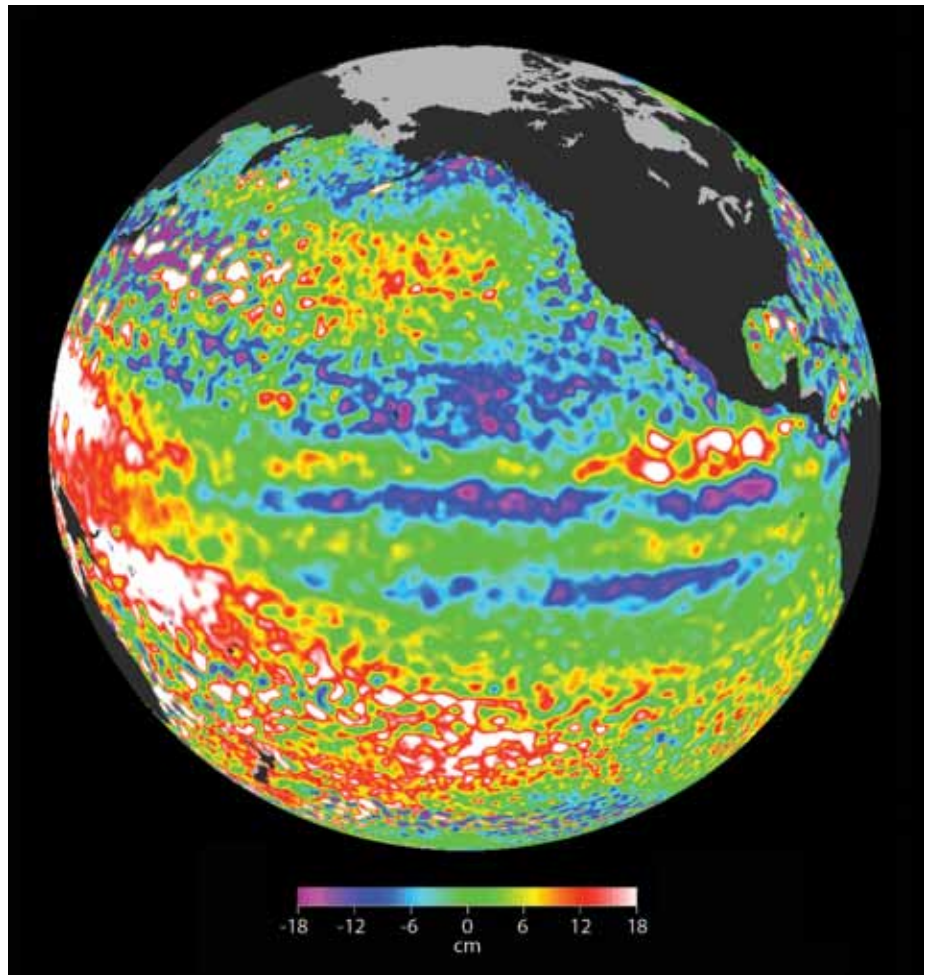

Figure 1. Sea surface height anomalies on April 8, 2009, in the Pacific Ocean from the AVISO merged data set.

Le Traon and Dibarboure (2002) provided a summary of the mapping capabilities of the T/P + ERS (Jason-1 + Envisat) configuration, using simulations from a high-resolution ocean general circulation model. With two altimeters in the T/P-ERS configuration, they found that sea level could be mapped with an accuracy of better than 10% of signal variance, while velocity can be mapped with an accuracy of 20–40% of signal variance (depending on latitude). A large part of the mapping error is due to unresolved high-frequency, high-wavenumber signals. Although the T/P + ERS merged data set has provided a much better representation of mesoscale variability than previous results, it is far from fully resolving mesoscale variability. From October 2002 to September 2005, there was an exceptional sampling of the ocean with four altimeter missions flying simultaneously (Jason-1, ERS-2, T/P interleaved with Jason-1, and Geosat Follow-On [GFO]). Pascual at al. (2006) merged these data sets to improve estimation of mesoscale surface circulation. They showed that the combination of

---

[1] Segment Sol multimissions d'ALTimétrie, d'Orbitographie et de localisation precise/Data Unification and Altimeter Combination System

Jason-1 + ERS-2 alone failed to reproduce many small-scale signals. In areas of intense variability, the root-mean-square (rms) differences between SSH maps from two altimeters and those from four altimeters reach up to 10 cm and 400 (cm s^{-1})^2 in SSH and eddy kinetic energy (EKE), respectively.

Tracking Eddies

The improved spatial resolution of SSH fields in the AVISO merged data revealed the prevalence of mesoscale eddies throughout most of the world's ocean. Thousands of eddies can be identified globally at any given time (Chelton et al., 2007, in press). Investigation of the characteristics of this large number of eddies thus mandates the use of automated procedures to identify the eddy positions, to estimate their amplitudes and scales, and to determine their trajectories.

The first automated procedure for detection and tracking of eddies in altimeter data was developed by Isern-Fontanet et al. (2003), building upon techniques developed previously for turbulence studies from numerical model simulations (e.g., Okubo, 1970; Weiss, 1990). Subsequent studies have fine-tuned the methodology to address various shortcomings (e.g., Morrow et al., 2004; Chaigneau et al., 2008; Chelton et al., 2007, in press). The procedures strive to identify eddies as compact structures in SSH or in variables related to the relative vorticity field that are intended to isolate rotating features. In altimetric applications, vorticity-based methods are not as well suited as SSH-based methods because they require computation of SSH derivatives, which amplify any noise that exists in the SSH field (Chelton et al., in press). After

the eddies are identified in each SSH field, an automated procedure is applied to determine the trajectory of each eddy.

The eddy trajectories confirm that eddies occur nearly everywhere in the world's ocean (Figure 2a). There are 6% more cyclones than anticyclones with lifetimes ≥ 16 weeks (18,469 and 17,422, respectively). A detailed analysis, however, finds that the eddies with the longest lifetimes and longest propagation distances are predominantly anti-cyclonic. Approximately three-fourths of the eddies in Figure 2a had net westward displacement; the 8600 eddies with net eastward displacement were confined to regions of strong eastward currents that advect the eddies downstream. SSH is typically influenced by four to six eddies per year within the eddy-rich regions and two to three eddies per year in the more quiescent regions. Very few eddies were observed in the region of the Northeast Pacific Ocean centered near 50°N, 160°W, and in an analogous region of the Southeast Pacific Ocean near 50°S, 95°W. If eddies exist in these regions, their amplitudes or scales are too small to be detected in the AVISO maps for the 16-week minimum lifetime considered here. The apparent small number of eddies in the tropics is attributable mostly to technical difficulties in identifying and tracking low-latitude eddies because of their fast propagation speeds, large spatial scales, and the rapid evolution of their structures.

With the exceptions of a few localized regions, eddies form nearly everywhere in the world's ocean. Formation rates are highest in eastern boundary current systems. The essentially global geographical distribution of eddy origins supports the conclusions of past

studies that the generation mechanism is likely baroclinic instability of the vertically sheared ocean currents, especially in regions where the flow has a nonzonal component (Smith, 2007, and references therein).

The mean amplitudes of the eddies vary considerably geographically (Figure 2b). The largest eddies are found in regions of strong, meandering currents (western boundary currents and their extensions into the ocean interior, the Antarctic Circumpolar Current, and the Loop Current in the Gulf of Mexico), where the mean amplitudes can exceed 30 cm. The mean amplitudes are moderately large in some eastern boundary current regions (e.g., the California Current and the Leeuwin Current off the west coast of Australia), in the eastern tropical Pacific in association with the Central American wind jets, in the subtropical western North and South Pacific, and in a few other regions. The mean amplitudes are only a few centimeters in the ocean interiors away from regions of energetic mesoscale variability.

The mean radius scales of the eddies decrease approximately monotonically from about 200 km near the equator to about 75 km at 60° latitude (Figure 2c). At mid and high latitudes, these scales are much larger than the baroclinic Rossby radius of deformation at which energy is input to the ocean from baroclinic instability. The larger scales of the eddies is consistent with the up-scale transfer of energy that is expected from surface quasi-geostrophic turbulence theory (e.g., Capet et al., 2008).

A key feature of observed mesoscale eddies that distinguishes them from linear Rossby waves is their degree of nonlinearity, which can be assessed by

a variety of metrics. One useful metric is the ratio of the maximum rotational fluid velocity U within the interior of an eddy to its translation speed c. (Note that both U and c are estimated from SSH anomalies and are thus relative to the mean flow.) When this nondimensional parameter U/c exceeds 1, there is trapped fluid within the eddy interior (Samelson and Wiggins, 2006). The eddy can then transport heat, salt, and biogeochemical properties such as nutrients and phytoplankton. Nonlinear eddies can thus have important influences on heat flux and marine ecosystem dynamics, in addition to their well-established importance in momentum and energy fluxes. The mean value of U/c exceeds 1 everywhere poleward of about 20° latitude in both hemispheres, reaching values higher than 15 in eddy-rich regions (Figure 2d). A detailed analysis finds that more than 99% of extratropical eddies were nonlinear by this metric (Chelton et al., in press). Many were highly nonlinear, with 48% having $U/c > 5$ and 21% having $U/c > 10$. Although U/c is smaller in the tropics where the translation speeds c become high, even there more than 90% of the eddies had $U/c > 1$.

Additional evidence for nonlinearity of the observed mesoscale eddies is the consistency of their propagation speeds and directions with theoretical predictions for large, nonlinear eddies (McWilliams and Flierl, 1979; Cushman-Roisin et al., 1990). In particular, westward propagation speeds are very near the phase speed of nondispersive baroclinic Rossby waves, and 84% of the eddies that propagated more than 1000 km had average azimuths that differed by less than 15° from due west. Also consistent with theory, there are
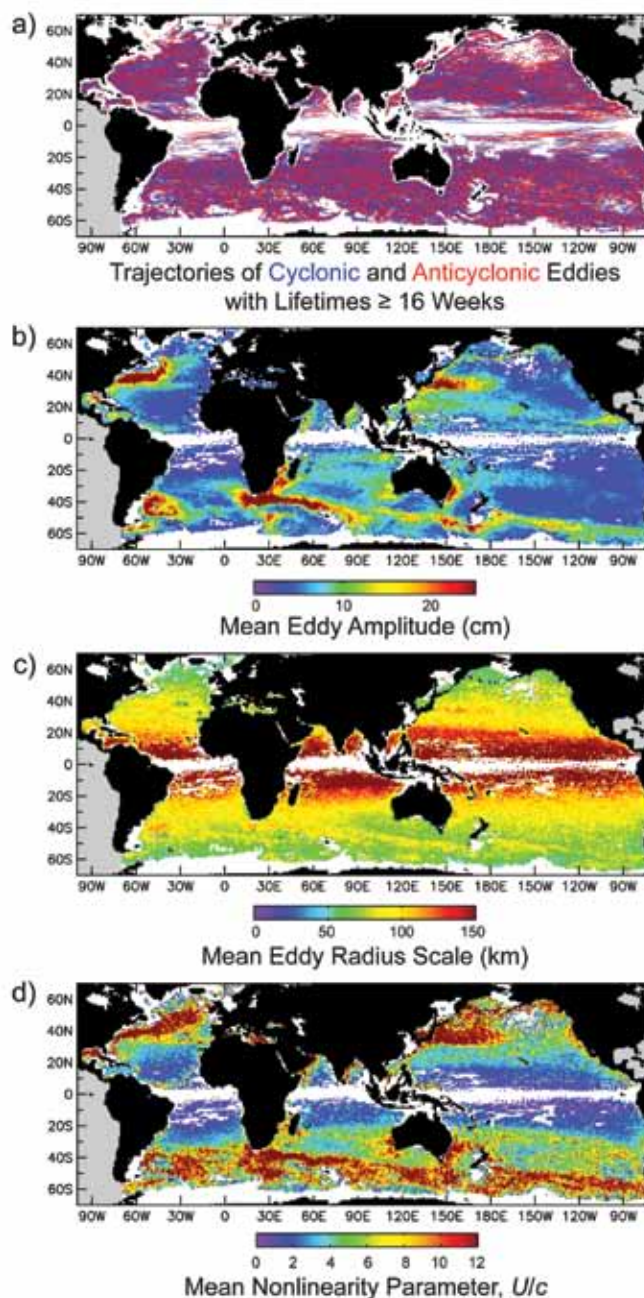
small opposing meridional deflections of cyclones and anticyclones (poleward and equatorward, respectively), as first noted regionally by Morrow et al. (2004) and shown globally by Chelton et al. (2007, in press).

The wealth of information about mesoscale eddies in the AVISO merged data set is enabling studies of the kinematics and dynamics of mesoscale

Figure 2. Global maps of eddy characteristics that were tracked for 16 weeks or longer in the first 16 years of the merged data set (October 1992– December 2008): (a) trajectories of cyclonic and anticyclonic eddies (blue and red lines, respectively); (b) mean amplitude for each 1° square; (c) mean scale for each 1° square, defined to be the effective radius at which the rotational speed averaged around an SSH contour is maximum; and (d) mean nonlinearity parameter U/c (see text). *Adapted from Chelton et al. (in press)*

eddies that have not previously been possible. While the altimeter observations provide unprecedented coverage of the surface characteristics of the eddies, many important questions about their significance in ocean dynamics and thermodynamics, as well as their role in marine ecosystem dynamics, require subsurface information as well. These questions are being addressed in ongoing

research using analysis of the altimetric SSH fields in conjunction with subsurface float observations and ocean general circulation models.

An Eulerian Description of Eddy Propagation

While the tracking of individual isolated eddies summarized in the last section was performed by following eddy trajectories in a Lagrangian manner, global eddy propagation can also be characterized in an Eulerian framework. Kuragano and Kamachi (2000), Jacobs et al. (2001), and Brachet et al. (2004) fitted certain functional forms to eddy covariance to estimate eddy propagation velocity. The decade-long SSH time series available on AVISO grids allows direct computation of eddy covariance at a given location and searches for the maximum correlation in space and time lags. Using such an approach, Fu (2009) provided a global description of the pattern and velocity of the propagation of eddy variability. Propagation velocity is highly inhomogeneous in space. Outside the equatorial zone, zonal propagation is intrinsically westward, modified by ocean currents, which could reverse the zonal eastward propagation in regions like the Gulf Stream and the Antarctic Circumpolar Current (ACC).

Figure 3 shows an example of the effects of currents and bottom topography on eddy propagation for a sector of the Southern Ocean (Fu, 2009). Eastward propagation is generally seen along the paths of the ACC, represented by the paths of the Sub-Antarctic Front (SAF) and the Polar Front (PF). In the western part of the region, eddy propagation generally follows the two fronts located between 45°S and 50°S until they cross over the Southwest Indian Ridge at 30°E, 50°S, where a sharp bifurcation of eddy propagation occurs, with one branch moving southward and the other continuing eastward and northeastward. A similar bifurcation of the two fronts takes place just east of the ridge. Topographic influences of the Conrad Rise at 45°E, 53°S and the Del Cano Rise at 45°E, 45°S are prominent. The Kerguelen Plateau also exerts a significant effect on eddy propagation, causing acceleration of eastward propagation both north and south of the plateau.

The blue line in Figure 4 shows the latitudinal profile of the zonal averages of the westward propagation speeds estimated by the Eulerian method. The results are in very close agreement, with the westward propagation speeds estimated by the Lagrangian method from the tracked eddies summarized in the previous section (the red line in Figure 4).

FLUX OF OCEANIC ENERGY AND PROPERTIES

Ocean eddies provide an important mechanism for transporting heat, salt, and nutrients in the ocean. Although the fraction of eddy transport in the total meridional heat transport is quite small in the ocean interior, eddy heat transport plays an important role in the
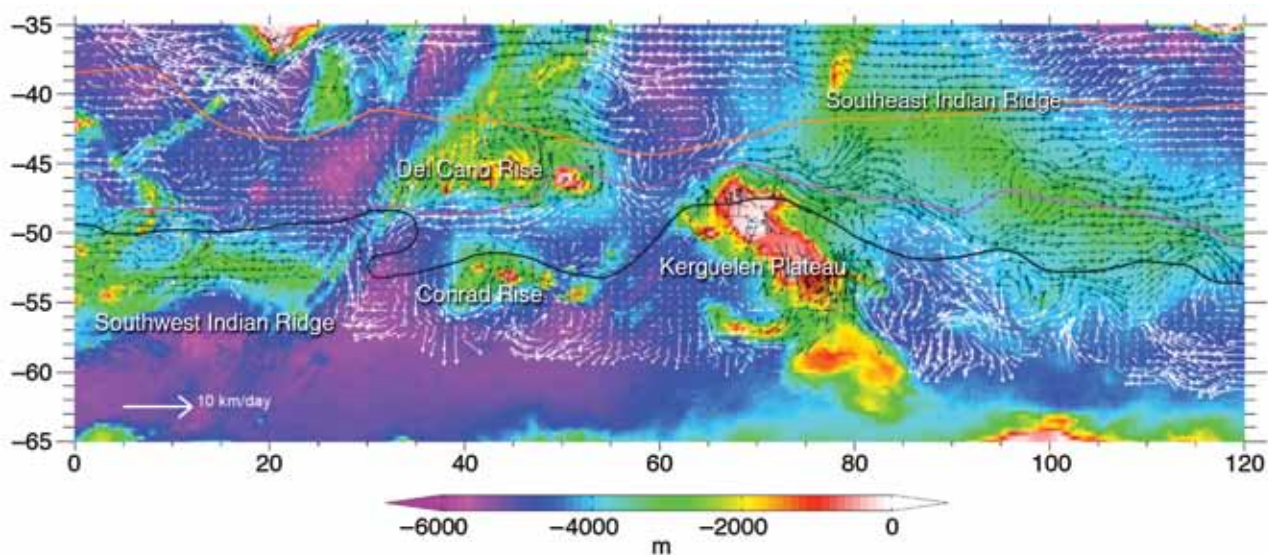

Figure 3. The velocity of eddy propagation in the Southern Ocean between 0° and 120°E, superimposed on ocean bathymetry. The different colors of the arrows are for ease of viewing. The three colored curves are (from north to south) the Subtropical Front, the Sub-Antarctic Front, and the Polar Front, respectively. *From Fu (2009)*

heat balance of strong western boundary currents, the ACC, and the tropical ocean (Wunsch, 1999). Holloway (1986) provided the first demonstration of using satellite altimetry to estimate the spatial pattern of eddy heat transport. He applied geostrophic turbulence theory to the standard deviation of global SSH obtained from Seasat altimeter data for estimating eddy diffusivity, which was then multiplied by the depth-averaged climatological gradient of temperature to compute eddy heat transport in the North Pacific Ocean. His results revealed a great deal of variability associated with the Kuroshio Current.

Using multiple years of T/P data with an alternative approach, Stammer (1998) computed meridional transport of heat and salt in the global ocean. He argued that eddy diffusivity is proportional to the product of eddy velocity and a length scale related to eddy kinetic energy and time scales, which both can be derived from satellite altimetry data. The eddy diffusivity was used with the mean meridional gradient of temperature and salinity, obtained from hydrographic data, to compute the mean meridional transport of heat and salt. Stammer (1998) illustrated that eddy diffusivity was highly inhomogeneous in the global ocean, reaching 2500 m^2 s^{-1} in the energetic western boundary currents and the tropical zonal currents, and decreasing to 250 m^2 s^{-1} in the ocean interior and eastern basins. His calculation of the meridional eddy transports of heat and salt also have a high degree of spatial inhomogeneity. Substantial poleward transports of heat and salt occur in the energetic western boundary currents: the Gulf Stream, Kuroshio, and Agulhas. Equatorward transports
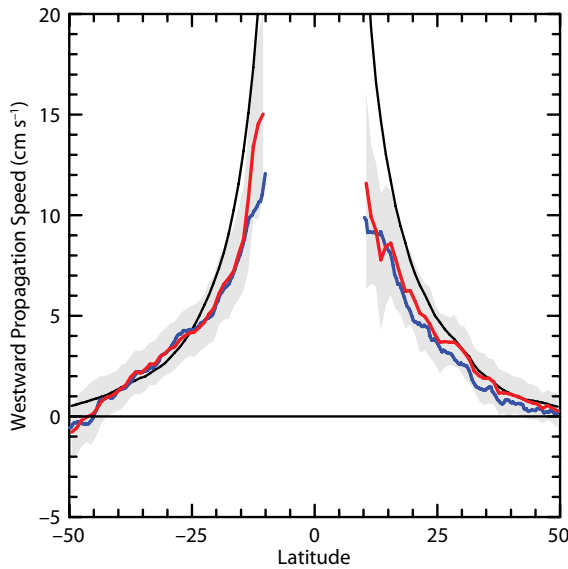

Figure 4. Latitudinal profile of the global zonal average of the propagation speeds of all the eddies with lifetimes ≥16 weeks obtained by Chelton et al. (in press) based on the eddy tracking method (red line). The gray shading indicates the 25 and 75 percentile points of the distribution of speeds along each latitude. The blue line is the latitudinal profile of the global zonal average of the eddy propagation speeds estimated from space-time lagged cross-correlation analysis by Fu (2009). The black line is the latitudinal profile of the zonally averaged westward phase speeds of nondispersive baroclinic Rossby waves.

are found between 5° and 15° latitude in the tropics.

The weakness of estimating eddy transports using the methods of Holloway (1986) and Stammer (1998) was discussed by Qiu and Chen (2005), who pointed out that eddy transports were not always down gradient of temperature and salinity as implied in the altimetric approach, and that the vertical structure of temperature and salinity had been ignored. Combining altimeter data with satellite sea surface temperature data and vertical temperature profiles from Argo floats to estimate eddy heat transport in the subtropical North Pacific, they obtained meridional eddy heat transport that was somewhat less than the altimetric estimates. The importance of subsurface information for determining eddy heat transport was also noted by Roemmich and Gilson (2001), who showed that a vertical tilt of the eddy core was essential for eddy transport of heat.

Eddy diffusivity has also been studied using dispersion statistics obtained from surface drifters or numerically

simulated floats based on surface currents derived from altimetry. The spatial-temporal coverage of the altimetric surface currents allows one to test different statistical techniques to estimate eddy diffusivity. This is a field of active research (e.g., Marshall et al., 2006; Sallée et al., 2008) because eddy diffusivity has important impacts on ocean mixing. In addition, altimeter-derived estimates can be used to test and develop new model parameterizations of eddy diffusivity.

Energy flux through different spatial scales, or energy cascade, is a fundamental problem in ocean dynamics, addressing the sources and sinks of ocean circulation energy. At oceanic mesoscales, a well-established theory for energy cascade is quasi-geostrophic turbulence (Rhines, 1977). This theory predicts that the baroclinic energy (with vertically varying structure) in the ocean tends to cascade from both small and large scales toward the deformation radius of the first baroclinic mode (10–100 km), where the energy is converted into barotropic mode

(vertically uniform structure) and then the energy is cascaded into larger scales in a process called "inverse cascade." The theory has been illustrated with numerical models but has never been tested by observations until recently.

Scott and Wang (2005) made the first calculation of energy cascade in wavenumber space from satellite altimeter data. Their results revealed an inverse cascade at scales larger than the deformation radius. Because altimetry observations are primarily the SSH perturbations associated with motions of the first baroclinic mode, the observed inverse cascade of baroclinic motions is not consistent with the Rhines (1997) theory, which allows inverse cascade only for barotropic modes at scales larger than the radius of deformation. The observed inverse cascade of baroclinic energy is thus puzzling from the standpoint of the conventional theory of quasi-geostrophic turbulence. However, the theory of surface quasi-geostrophic turbulence does provide a framework to explain the inverse cascade of upper-ocean baroclinic energy (Capet et al., 2008). Together with the findings of the $k^{-11/3}$ spectral slope described earlier, evidence of inverse cascade validates the theory of surface quasi-geostrophic turbulence for describing energy transfer in the upper ocean.

Qiu et al. (2008) applied the technique of Scott and Wang (2005) to study seasonal energy exchange between the mean flow and the eddy field of the Subtropical Counter Current in the South Pacific Ocean. They found that the instability of the mean flow generated meridionally elongated eddies that, through eddy-eddy interactions, transformed into zonally elongated

eddies. The energy was then transferred from eddy scales to larger zonal scales in an anisotropic inverse cascade process. This is probably the first observational evidence for the detailed mechanism of energy exchange between mean flow and eddy variability and the transformation of scales.

SMALL-SCALE PROCESSES AND THE FUTURE CHALLENGE IN SATELLITE ALTIMETRY

The resolution limit of the currently available altimeter data set raises many issues. Most of the swift currents in the ocean have cross-stream widths in the range of 10–100 km, which are not fully resolved in the gridded AVISO maps. Along-track altimeter data can now be processed to reveal strong fronts and coastal currents with scales of 50–100 km, but we cannot observe these features between the ground tracks. Higher-resolution data sets are needed to fully resolve their details.

Limited in situ measurements of temperature, salinity, and velocity, and high-resolution satellite measurements

of ocean color, sea surface temperature, and synthetic aperture radar imagery, have shown the prevalence of fronts and filaments in the ocean at scales shorter than 100 km, and their importance in mixing and transporting ocean heat and nutrients. It is estimated that about 50% of the vertical transport of ocean biogeochemical properties takes place at these small scales (Lapeyre and Klein, 2006).

Numerical model experiments suggest that the three-dimensional structure of upper ocean circulation at these scales can be estimated from high-resolution SSH information based on surface quasi-geostrophic turbulence theory (Klein et al., 2009). Figure 5 compares model-simulated vertical velocity and vorticity of the upper ocean to reconstructions from the theory, illustrating the efficacy of high-resolution SSH observations for studying vertical transfer processes in the ocean. Furthermore, the processes taking place at these scales are critical to understanding the balance of the kinetic energy of ocean circulation, involving both inverse and forward energy cascades (Capet et al., 2008).
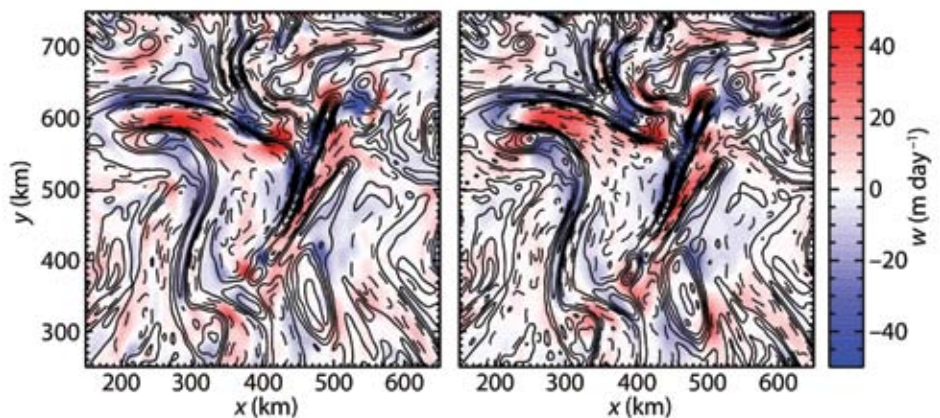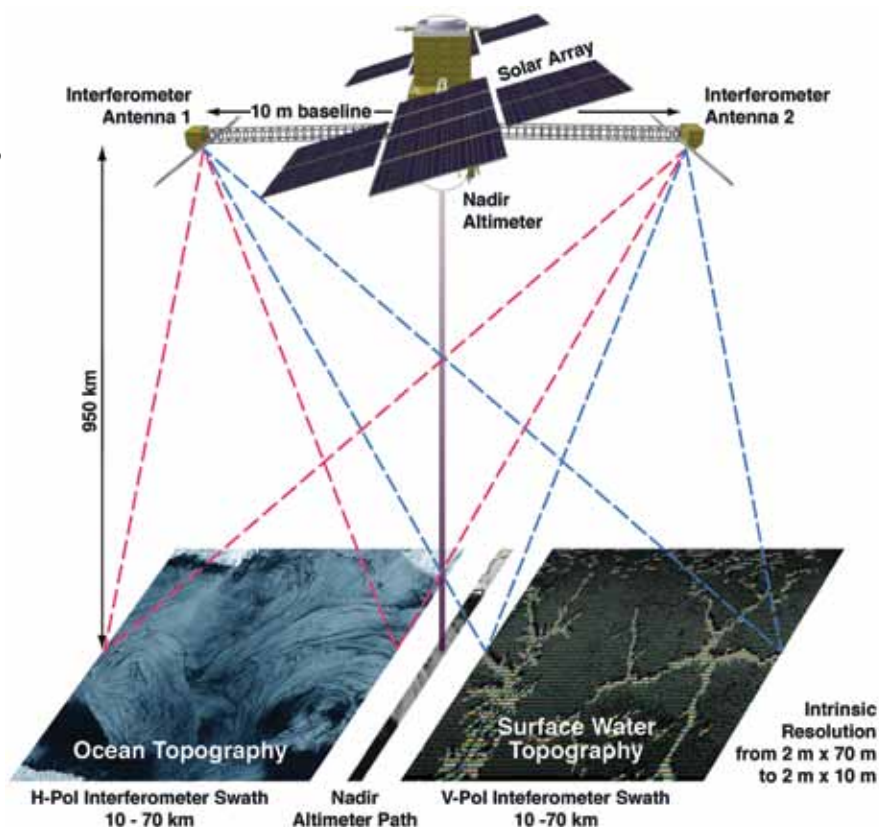

Figure 5. (left) Model-simulated low-frequency vertical velocity (in colors) and relative vorticity (contours) at 200 m. (right) Reconstructed vertical velocities (in colors) and relative vorticity (contours) at 200 m from sea surface height using surface quasi-geostrophic theory. *From Klein et al. (2009)*

THE SURFACE WATER AND OCEAN TOPOGRAPHY MISSION

The figure (right) illustrates the measurement principle of the SWOT mission. Two synthetic-aperture radar (SAR) antennae are mounted on the two ends of a mast about 10-m long. Each antenna looks sideways with a small off-nadir angle of about 4°, illuminating a swath 60-km wide across the flight direction on each side of the spacecraft. The two antennae simultaneously receive radar signals reflected by the rough sea surface. The phase differences between the two signals allow interferometric calculation of the off-nadir angle of the received signals. The combined information of the off-nadir angle, the range of the reflecting sea surface from the radar measurement, and the spacecraft altitude from orbit determination allows estimation of sea surface height relative to an Earth-fixed coordinate.

Configuration of a wide-swath altimetry mission based on the radar interferometry technique.

The intrinsic resolution of SAR is on the order of a few meters, allowing high spatial resolution of the measurement. To achieve the low measurement noise required for observing oceanic signals, the radar frequency was chosen in the Ka band (about 35 GHz). However, the noise level of the raw measurement, on the order of 10 cm, is still too high for observing oceanic submesoscales. After smoothing over a large number of raw measurements, random measurement noise can be reduced to a level of 1 cm over 1 km x 1 km resolution cells. This measurement performance is nearly two orders of magnitude better than that of Jason-1 (Fu and Ferrari, 2008). SWOT observations are expected to resolve ocean variability at wavelengths of 10–25 km.

Within 10 km of the nadir path, the ranges of the signals received by the two SAR antennae are too close to each other for interferometric calculations, leaving a 20-km gap in the swath measurement. An option under consideration is to carry a conventional altimeter for making nadir observations. Although the spatial resolution is limited, the nadir observations are useful for calibrating the interferometry observations to minimize systematic errors at large scales for studying the interaction of submesoscale processes with large-scale ocean circulation. Other payloads of such a mission include a multifrequency microwave radiometer to correct for the errors caused by tropospheric water vapor, as well satellite tracking sensors for precision orbit determination. Because the sensitivity of radar measurements to ionospheric free electrons is very weak at Ka-band frequencies, the dual-frequency corrections for ionospheric effects that were necessary for the accurate measurements obtained from T/P and Jason-1 and -2 are not required for SWOT.

To make fundamental advances toward improving ocean circulation models for studying future climate evolution, observations at wavelengths of 10–100 km are needed to address the small end of the mesoscale, loosely defined as the submesoscale here (the term has also been used to refer to scales of 50 m–10 km in other contexts). Use of radar interferometry for high-resolution, wide-swath SSH observations is being developed for the next-generation altimetry missions to meet the challenge of observing submesoscale ocean processes (Fu and Rodriguez, 2004; Fu and Ferrari, 2008).

The capability for high-resolution measurements of water surface elevation also makes the technique of wide-swath altimetry useful in land hydrology for observing the storage and discharge rates of land water bodies (Durand et al., 2010). Recognizing the need of high-resolution wide-swath altimetry for advancing both oceanography and land hydrology to address critical issues in climate change, the decadal survey conducted by the US National Research Council (NRC, 2007) recommended the flight of a mission called Surface Water and Ocean Topography (SWOT) to measure the water elevation of the global oceans as well as rivers and lakes on land. The US National Aeronautics and Space Administration (NASA) and the French space agency, Centre National d'Études Spatiales (CNES), are partnering to implement the SWOT mission. This mission will address two major issues of a warming climate: improving understanding of ocean circulation that holds the key to the warming rate, and improving the knowledge of shifting water resources resulting from the warming. SWOT will thus be a critical tool for observing the hydrosphere from space, and will set a standard for future satellite altimetry.

> "TO MAKE FUNDAMENTAL ADVANCES TOWARD IMPROVING OCEAN CIRCULATION MODELS FOR STUDYING FUTURE CLIMATE EVOLUTION, OBSERVATIONS AT WAVELENGTHS OF 10–100 KM ARE NEEDED..."

ACKNOWLEDGEMENTS

REFERENCES

Brachet, S., P.Y. Le Traon, and C. Le Provost. 2004. Mesoscale variability from a high-resolution model and from altimeter data in the North Atlantic Ocean. *Journal of Geophysical Research* 109, C12025, doi:10.1029/2004JC002360.

Capet, X., P. Klein, B.L. Hua, G. Lapeyre, and J.C. McWilliams. 2008. Surface kinetic energy transfer in surface quasi-geostrophic flows. *Journal of Fluid Mechanics* 604:165–174.

Chaigneau, S., A. Gizolme, and C. Grados. 2008. Mesoscale eddies off Peru in altimeter records: Identification algorithms and eddy spatio-temporal patterns. *Progress in Oceanography* 79:106–119.

Charney, J.G. 1971. Geostrophic turbulence. *Journal of Atmospheric Science* 28:1,087–1,095.

Chelton, D.B., M.G. Schlax, R.M. Samelson, and R.A. de Szoeke. 2007. Global observations of large oceanic eddies. *Geophysical Research Letters* 34, L15606, doi:10.1029/2007GL030812.

Chelton, D.B., M.G. Schlax, and R.M. Samelson. In press. Global observations of nonlinear mesoscale eddies. *Progress in Oceanography*.

Cheney, R.E., J.G. March, and B.D. Beckley. 1983. Global mesoscale variability from collinear tracks of Seasat altimeter data. *Journal of Geophysical Research* 88:4,343–4,354.

Cushman-Roisin, B., E.P. Chassignet, and B. Tang. 1990. Westward motion of mesoscale eddies. *Journal of Physical Oceanography* 20:758–768.

Ducet, N., P.Y. Le Traon, and G. Reverdin. 2000. Global high resolution mapping of ocean circulation from the combination of TOPEX/POSEIDON and ERS-1/2. *Journal of Geophysical Research* 105:19,477–19,498.

Durand, M., L.-L. Fu, D.P. Lettenmaier, D.E. Alsdorf, E. Rodrigues, and D. Esteban-Fernandez. 2010. The Surface Water and Ocean Topography mission: Observing terrestrial surface water and oceanic submesoscale eddies. *Proceedings of IEEE 98(5):766–779*.

Fu, L.-L. 1983. On the wavenumber spectrum of oceanic mesoscale variability observed by the Seasat altimeter. *Journal of Geophysical Research* 88:4,331–4,341.

Fu, L.-L. 2009. Pattern and velocity of propagation of the global ocean eddy variability. *Journal of Geophysical Research* 114, C11017, doi:10.1029/2009JC005349.

Fu, L.-L., and R. Ferrari. 2008. Observing oceanic submesoscale processes from space. *Eos, Transactions, American Geophysical Union* 89(48):488.

Fu, L.-L., and R. Rodriguez. 2004. High-resolution measurement of ocean surface topography by radar interferometry for oceanographic and geophysical applications. Pp. 209–224 in *State of the Planet: Frontiers and Challenges*. R.S.J. Sparks and C.J. Hawkesworth, eds, AGU Geophysical Monograph 150, IUGG Vol. 19.

Holloway, G. 1986. Estimation of oceanic eddy transports from satellite altimetry. *Nature* 323:243–244, doi:10.1038/323243a0.

Huang, N.E., C.D. Leitao, and C.G. Para. 1978. Large-scale Gulf Stream frontal study using GEOS3 radar altimeter data. *Journal of Geophysical Research* 83:4,673–4,682.

Isern-Fontanet, J., E. Garcia-Ladona, and J. Font. 2003. Identification of marine eddies from altimetric maps. *Journal of Atmospheric and Oceanic Technology* 20:772–778.

Jacobs, G.A., C.N. Barron, and R.C. Rhodes. 2001. Mesoscale characteristics. *Journal of Geophysical Research* 106:19,581–19,595.

Klein, P., J. Isern-Fontanet, G. Lapeyre, G. Roullet, E. Danioux, B. Chapron, S. Le Gentil, and H. Sasaki. 2009. Diagnosis of vertical velocities in the upper ocean from high-resolution sea surface height. *Geophysical Research Letters* 36, L12603, doi:10.1029/2009GL038359.

Kuragano, T., and M. Kamachi. 2000. Global statistical space-time scales of oceanic variability estimated from the TOPEX/POSEIDON altimeter data. *Journal of Geophysical Research* 105(C1):955–974.

Lapeyre, G., and P. Klein. 2006. Impact of the small-scale elongated filaments on the oceanic vertical pump. *Journal of Marine Research* 64:835–851.

Le Traon, P.-Y., and R. Morrow. 2001. Ocean currents and eddies. Pp. 171–210 in *Satellite Altimetry and Earth Sciences: A Handbook for Techniques and Applications*. L.-L. Fu and A. Cazenave, eds, Academic Press, San Diego.

Le Traon, P.-Y. 1993. Comment on "Mesoscale variability in the Atlantic ocean from Geosat altimetry and WOCE high resolution numerical modeling by D. Stammer and C.W. Böning." *Journal of Physical Oceanography* 23:2,729–2,732.

Le Traon, P.-Y., and G. Dibarboure. 2002. Velocity mapping capabilities of present and future altimeter missions: The role of high frequency signals. *Journal of Atmospheric and Oceanic Technology* 19:2,077–2,088.

Le Traon, P.-Y., F. Nadal, and N. Ducet. 1998. An improved mapping method of multi-satellite altimeter data. *Journal of Atmospheric and Oceanic Technology* 15:522–534.

Le Traon, P.-Y., P. Klein, B.L. Hua, and G. Dibarboure. 2008. Do altimeter data agree with interior or surface quasi-geostrophic theory? *Journal of Physical Oceanography* 38(5):1,137–1,142.

Marshall, J., E. Shuckburgh, H. Jones, and C. Hill. 2006. Estimates and implications of surface eddy diffusivity in the Southern Ocean derived from tracer transport. *Journal of Physical Oceanography* 36:1,806–1,821.

McWilliams, J.C., and G.R. Flierl. 1979. On the evolution of isolated, nonlinear vortices. *Journal of Physical Oceanography* 9:1,155–1,182.

Morrow, R.A., R. Coleman, J.A. Church, and D.B. Chelton. 1994. Surface eddy momentum flux and velocity variance in the Southern Ocean from GEOSAT altimetry. *Journal of Physical Oceanography* 24:2,050–2,071.

Morrow, R., F. Birol, D. Griffin, and J. Sudre. 2004. Divergent pathways of cyclonic and anti-cyclonic ocean eddies. *Geophysical Research Letters* 31, L24311, doi:10.1029/2004GL020974.

NRC (National Research Council). 2007. *Earth Science and Applications from Space: National Imperatives for the Next Decade and Beyond.* Committee on Earth Science and Applications from Space: A Community Assessment and Strategy for the Future, National Academies Press, Washington, DC, 456 pp.

Okubo, A. 1970. Horizontal dispersion of float-able particles in the vicinity of velocity singularities such as convergences. *Deep-Sea Research* 17:445–454.

Pascual, A., Y. Faugere, G. Larnicol, and P.-Y. Le Traon. 2006. Improved description of the ocean mesoscale variability by combining four satellite altimeters. *Geophysical Research Letters* 33, L02611, doi:10.1029/2005GL024633.

Qiu, B., and S. Chen. 2005. Eddy-induced heat transport in the subtropical North Pacific from Argo, TMI, and altimetry measurements. *Journal of Physical Oceanography* 35:458–473.

Qiu, B., R.B. Scott, and S. Chen. 2008. Length scales of eddy generation and nonlinear evolution of the seasonally modulated South Pacific Subtropical Countercurrent. *Journal of Physical Oceanography* 38(7):1,515–1,528.

Rhines, P.B. 1977. The dynamics of unsteady currents. Pp. 189–318 in *The Sea,* vol. 6. E.D. Goldberg, I.N. McCave, J.J. O'Brien, and J.H. Steele, eds, John Wiley and Sons.

Robinson, A.R., ed. 1983. *Eddies in Marine Science.* Springer-Verlag, 609 pp.

Roemmich, D., and J. Gilson. 2001. Eddy transport of heat and thermocline waters in the North Pacific: A key to interannual/decadal climate variability? *Journal of Physical Oceanography* 31:675–687.

Sallée, J.B., K. Speer, R. Morrow, and R. Lumpkin. 2008. An estimate of Lagrangian eddy statistics and diffusion in the mixed layer of the Southern Ocean. *Journal of Marine Research* 66(4):441–463.

Samelson, R.M., and S. Wiggins. 2006. *Lagrangian Transport in Geophysical Jets and Waves.* Springer-Verlag, New York, 147 pp.

Schlax, M.G., and D.B. Chelton. 2003. The accuracies of crossover and parallel-track estimates of geostrophic velocities from TOPEX/POSEIDON and Jason altimeter data. *Journal of Atmospheric and Oceanic Technology* 20:1,196–1,211.

Scharffenberg, M.G., and D. Stammer. 2010. Seasonal variations of the large-scale geostrophic flow field and eddy kinetic energy inferred from the TOPEX/Poseidon and Jason-1 tandem mission data. *Journal of Geophysical Research* 115, C2, doi:10.1029/2008JC005242

Scott, R.B., and F. Wang. 2005. Direct evidence of an oceanic inverse kinetic energy cascade from satellite altimetry *Journal of Physical Oceanography* 35(9):1,650–1,666.

Smith, K.S. 2007. The geography of linear baro-clinic instability in Earth's oceans. *Journal of Marine Research* 65:655–683.

Stammer, D. 1997. Global characteristics of ocean variability estimated from regional TOPEX/POSEIDON altimeter measurements. *Journal of Physical Oceanography* 27:1,743–1,769.

Stammer, D. 1998. On eddy characteristics, eddy transports, and mean flow properties. *Journal of Physical Oceanography* 28:727–739.

Weiss, J. 1991. The dynamics of enstrophy transfer in two-dimensional hydrodynamics. *Physica D* 48:273–294.

Wunsch, C. 1999. Where do ocean eddy heat fluxes matter? *Journal of Geophysical Research* 104:13,235–13,249.

Zlotnicki, V., L.-L. Fu, and W. Patzert. 1989. Seasonal variability in a global sea level observed with GEOSAT altimetry. *Journal of Geophysical Research* 94:17,959–17,969.